

Received 27 January 2024, accepted 19 February 2024, date of publication 22 February 2024, date of current version 1 March 2024.

Digital Object Identifier 10.1109/ACCESS.2024.3368884



RESEARCH ARTICLE

Demonstration of 120 Gbit/s 64-QAM Wireless Link Operating in the 300 GHz Band

IRSHAAD FATADIN¹⁰, (Senior Member, IEEE), JESS SMITH¹, YUNSONG GUI¹⁰, INGO NICKELEIT¹⁰, JAE PARK³, AND JEFFREY L. HESLER³, (Fellow, IEEE)

Corresponding author: Irshaad Fatadin (irshaad.fatadin@npl.co.uk)

This work was supported by the U.K. Government's Department for Science, Innovation, and Technology (DSIT) at the National Physical Laboratory (NPL).

ABSTRACT This paper demonstrates a 120 Gbit/s 64-Quadrature Amplitude Modulation (64-QAM) transmission link using all-electronics sub-harmonic mixers for the transmitter and the receiver operating in the 300 GHz band. The wireless signal is propagated through a non-line-of-sight free space link where reflections from 2 mirrors provide a channel length of 3 m over-the-air transmission between the transmitter and the receiver modules. Here, we demonstrate that an accurate correction of different error sources such as channel impairments of the 300 GHz wireless link as well as the combined effects of hardware amplitude and phase impairments can successfully be achieved for the high spectral-efficiency 64-QAM modulation scheme. The measured bit error ratio of the calibrated testbed is under the soft-decision forward error correction (SD-FEC) threshold of 2.7×10^{-2} up to 120 Gbit/s with 20% overhead giving a net data rate of 100 Gbit/s post-FEC. To the best of our knowledge, this is the highest 64-QAM performance achieved using an electronics-based transmitter in the 300 GHz band.

INDEX TERMS THz communications, 64-QAM, OTA transmission, digital signal processing, non-line-of-sight free space link.

I. INTRODUCTION

To support the continued exponential growth of data traffic in wireless networks, the THz band (0.3-10 THz) has attracted considerable attention where untapped frequency resources exist with the prospect of massive data capacity and connectivity [1], [2], [3], [4], [5], [6]. To date, the insatiable demand for more bandwidth has been accommodated over legacy wireless systems operating at lower frequency bands with advanced modulation schemes and signal processing technologies. However, without increasing the carrier frequencies to the THz band for more spectral resources, it will be challenging to keep up with the demand of bandwidth-hungry applications beyond 100 Gbit/s. In addition, short-range communication requirements for mobile video, holographic calls and machine-centric applications

The associate editor coordinating the review of this manuscript and approving it for publication was Angelo Trotta

such as Industry 4.0 are driving technological developments that can handle large amounts of data at increasing transfer rates [7]. For instance, streaming an uncompressed 8k video (assuming 7680 × 4320 resolution, 120 fps, 12-bits RGB per component) from a wireless beamer to a screen requires a data rate of 143.33 Gbit/s which can practically be achieved using a THz communication link whose prominent feature lies in the availability of large contiguous bandwidth [8]. However, limited by the available signal-to-noise ratio (SNR) in THz links with large bandwidths and channel impairments as well as linearity constraints of THz components, single-carrier transmission beyond 100 Gbit/s data rate is still very challenging with spectrally efficient modulation formats such as 64-OAM.

There are two complementary methods in the field of THz communications for generating high-speed wireless signals: photonics- and electronics-based techniques [9], [10]. In the photonics-based approach, a transmitter generates a

¹National Physical Laboratory (NPL), TW11 0LW Teddington, U.K.

²Keysight Technologies Deutschland GmbH, 71034 Böblingen, Germany

³Virginia Diodes Inc. (VDI), Charlottesville, VA 22902, USA

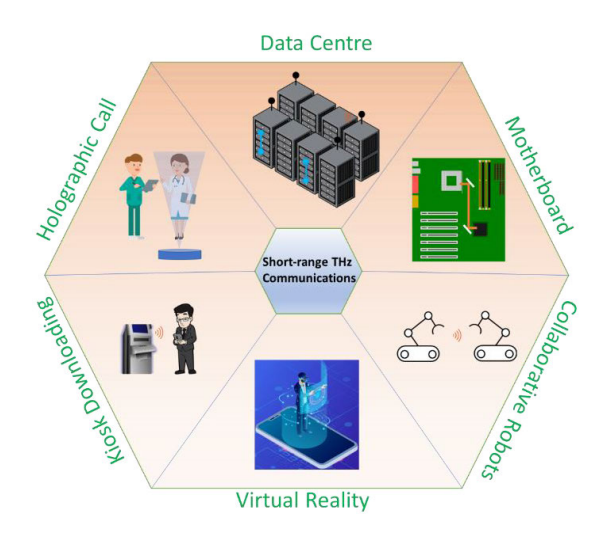


FIGURE 1. Prospective short-range target applications for THz communications. Different usage scenarios are shown for high-speed wireless communication link operating at THz frequencies requiring massive data capacity and connectivity. The support for futuristic scenarios is particularly considered, such as ubiquitous penetration of virtual reality, holographic telepresence and collaborative robots.

THz wireless signal by broadband photoelectric conversion using a high-speed uni-traveling-carrier photodiode (UTC-PD) [11], [12]. This approach is useful for THz-wireless bridge or fiber extender where it is not technically or economically viable to install optical fibers [13]. On the other hand, with the steadily increasing operation speed of transistors, electronics-based transmitters have attracted a lot of interest and are being actively investigated [14], [15]. Several transmitters using high-speed InP-based transistors have been reported as well as SiGe and CMOS-based technologies [16], [17], [18]. The all-electronics approach has the benefit of fulfilling all processes of signal handling in electronic circuits and is more established than the photonics-based counterpart regarding monolithic integrability and the potential for mass production. Our approach in this work was thus based on allelectronics up- and down-conversion of the wireless signal using sub-harmonic mixers for data transmission.

The high-capacity wireless link demonstrated in this paper has the potential to be deployed for short-range applications as shown in Figure 1 for different usage scenarios. These include device-to-device and rack-to-rack communications in a data centre environment to more futuristic scenarios such as ubiquitous penetration of augmented and virtual reality systems, collaborative robots and holographic telepresence. Moreover, transmission in the 300 GHz band is being actively investigated for rack-to-rack as well as intra-rack communications in data centers to support high connectivity for point-to-point and non-line-of-sight (NLoS) free space links [19], [20]. It is noted that in order to exploit the full capacity of the 300 GHz band, the use of spectrally efficient modulation formats such as 64-QAM is highly desirable to boost the transmission capacity within a given signal bandwidth [21], [22], [23], [24].

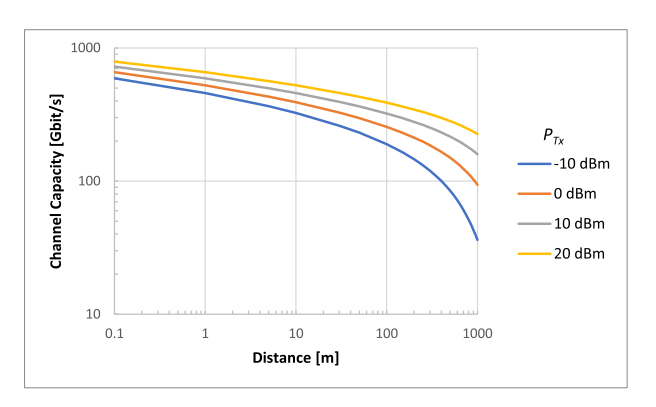


FIGURE 2. Channel capacity with transmission distance. The performance of a 300 GHz wireless link is presented using Shannon's theorem and free space path loss to compute the transmission distance for different transmitted power levels. The values of the parameters used in this calculation are shown in Table 1.

The paper is organized as follows. To begin with, the channel capacity of a 300 GHz link with transmission distance is evaluated based on Shannon's theorem. We then present the transmission setup with the transmitter and receiver based on a sub-harmonic mixer (SHM) architecture to perform frequency mixing. The intrinsic mixer conversion loss of the SHM used for the upconverter and the downconverter is presented. The characterization of the testbed using a vector signal analyzer (VSA) software is discussed for pre-emphasis equalization on the modulated signals at the transmitter. The digital signal processing (DSP) functional blocks used to compensate for post-transmission impairments on the received signals are also discussed including phase noise compensation. Finally, we present the 64-QAM transmission results from the 300 GHz wireless testbed using electronics-based transmitter and receiver modules and discuss the standardization effort in the field of THz communications.

II. CHANNEL CAPACITY WITH TRANSMISSION DISTANCE

From Shannon's theorem, the achievable channel capacity C is given by [25]

$$C = Blog_2\left(1 + \frac{S}{N}\right) \tag{1}$$

where, B is the channel bandwidth, S is the received signal power and N is the noise power. Given the large bandwidth available in the THz band, high data-rate wireless systems could be possible even though S generally tends to decrease for higher carrier frequency. The noise power in (1) is calculated in dBm using

$$N = 10log(KTB) + 30 + NF \tag{2}$$

where, $K = 1.38 \times 10^{-23}$ J/K is Boltzmann's constant, T is the absolute temperature in Kelvin, and NF is the noise figure of the receiver. The received signal power in (1) can be written as

$$S = P_{Tx} + G - FSPL - L_{atm} \tag{3}$$



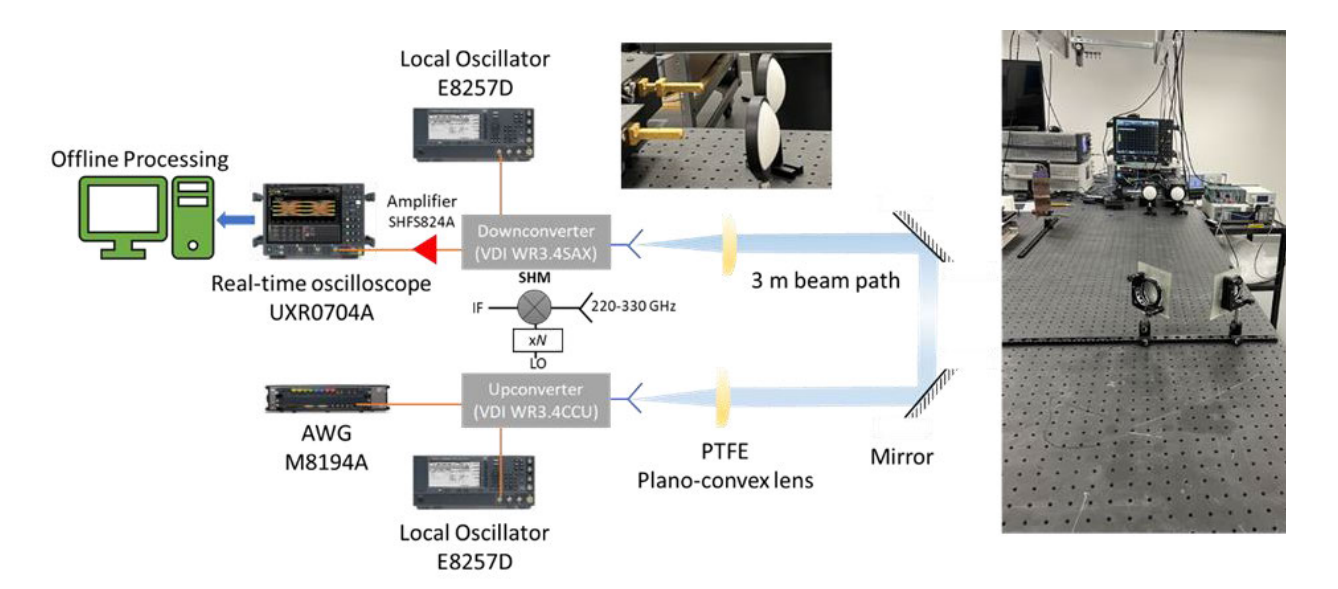


FIGURE 3. Experimental setup. The schematic for the short-range wireless transmission system in the 300 GHz band is shown. The high frequency signal is generated and detected using all-electronics mixers. The 3 m NLoS wireless distance was obtained through reflections on 2 mirrors as shown in the schematic setup. The data captured from the real-time oscilloscope is analyzed using offline processing to evaluate the performance of the transmission link. Photographs of the THz communication link system are also shown.

TABLE 1. Simulation parameters to calculate channel capacity with transmission distance.

Symbol	Quantity	Value
\overline{F}	Carrier frequency	300 GHz
G	Gain of antennas	100 dBi
B	Channel bandwidth	20 GHz
T	Absolute temperature	290 K
NF	Noise Figure	10 dB
L_{atm}	Atmospheric attenuation	5 dB/km

where, P_{Tx} is the transmitted power in dBm, G is the combined gain of the transmit and receive antennas, FSPL is the free space path loss and L_{atm} is the atmospheric attenuation (5 dB/km at 300 GHz). The free space path loss is calculated using the expression

$$FSPL = 20log(4\pi df/c) \tag{4}$$

where, d is the wireless transmission distance between the transmitter and the receiver, f is the carrier frequency and c is the speed of light. The FSPL is 91.5 dB for a transmission distance of 3 m at 300 GHz.

Using (1) – (4), we can compute the channel capacity with transmission distance. Figure 2 shows the simulation results at 300 GHz using the values in Table 1 for different transmitted power levels. As can be seen in Figure 2, the 300 GHz band has the potential to achieve significantly high transmission rates (beyond 100 Gbit/s) due to its much larger bandwidth available compared to lower frequency bands. For the 300 GHz band, the standard IEEE 802.15.3d has already proposed channel allocation from 252 GHz to 321 GHz. In addition, atmospheric attenuation is relatively low in this

transmission window. Therefore, research on the 300 GHz band has been attracting a lot of attention as a frequency band of choice for next-generation wireless communications [26], [27]. Moreover, broadband power amplifiers are being actively developed to further increase the practical transmission reach [28], [29].

III. EXPERIMENTAL SETUP

The experimental configuration is shown in Figure 3 using all-electronics transmitter and receiver modules supporting over-the-air transmission over the frequency range 220-330 GHz. We employed sub-harmonic mixers and high-level 64-QAM modulation to experimentally demonstrate BER under the SD-FEC limit up to 120 Gbit/s single-carrier transmission over a 3 m wireless distance. The M8194A 120 GSa/s arbitrary waveform generator (AWG) with an analog bandwidth of 45 GHz was used to generate the wide-bandwidth modulated intermediate frequency (IF) signals. A root-raised cosine filter (roll-off factor, $\alpha=0.22$) was applied to the 64-QAM baseband signals in order to reduce its spectral spread to fit within the bandwidth of the radio frequency (RF) modules and to minimize the influence of local oscillator (LO) spurs in the frequency spectrum.

A Virginia Diodes Inc (VDI) upconverter WR3.4CCU was used to convert the IF modulated signals from the AWG to the desired 300 GHz band. On the receive side, another VDI module WR3.4SAX was used as the downconverter for the over-the-air transmitted signals. Both of these conversion modules are based on Schottky diode SHMs, which allow conversion of wide bandwidth signals with relatively little distortion. The electrical LO signals for the VDI modules were generated using 2 Keysight E8257D PSG analog signal

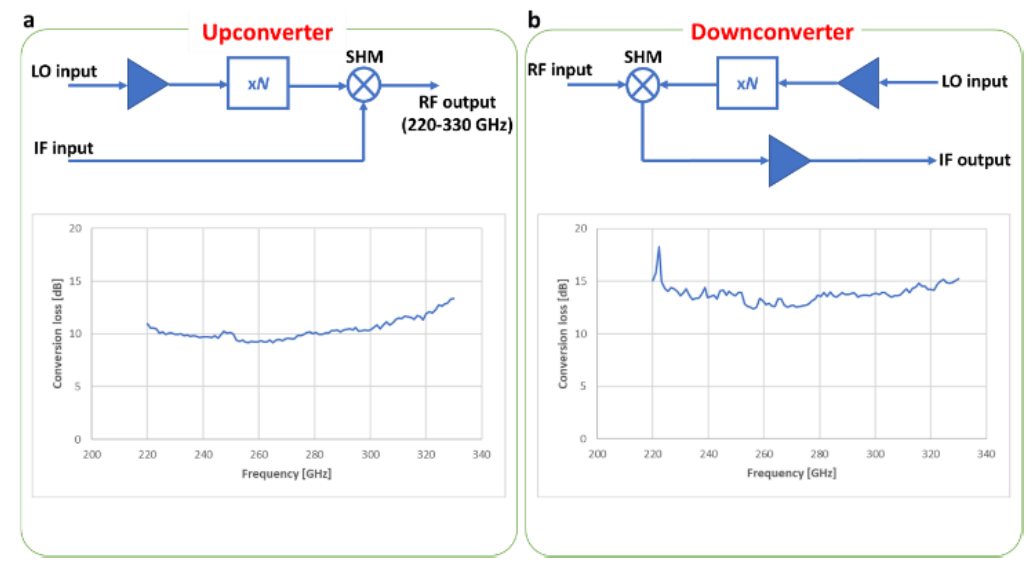


FIGURE 4. Sub-harmonic mixer characterisation results. Conversion loss of the SHM used to establish the 300 GHz datalink for the (a) upconverter and (b) downconverter. The intrinsic mixer conversion loss of the SHM was measured before IF amplification. The upconverter and the downconverter are both operational in the 220 - 330 GHz range by tuning the electrical LO signal to the desired carrier frequency for wireless transmission.

generators as illustrated in Figure 3. The PSGs have the option UNY to provide low phase noise for both the VDI upconverter and downconverter. For this experiment, the frequency of the PSGs was set at 25 GHz to drive the x12 LO generation paths of the VDI modules to give a desired carrier frequency of 300 GHz. By tuning the LO, any carrier frequency in the 220 - 330 GHz range can be achieved. The block diagrams of the transmitter and the receiver used to establish the wireless datalink are shown in Figure 4. The WR3.4 VDI modules can be tuned by sweeping the LO frequency from the analog signal generators. The characterization results for the intrinsic losses of the SHMs are shown in Figure 4 (a) and (b) for the upconverter and downconverter, which at 300 GHz are 10.4 dB and 13.8 dB, respectively. By adopting commercially available SHMs for both our transmitter and receiver, we significantly reduced the hardware complexity compared to photonics-based approaches where laser sources are employed to generate the sub-THz carrier frequency. By using an all-electronics system, we also avoid the higher level of phase noise inherent to laser sources which can be a significant factor inhibiting the performance of high-order modulation schemes.

As illustrated in Figure 3, the transmit and the receive modules were placed in a 3 m NLoS free space setup through reflections on 2 mirrors. The sub-THz signal is radiated into free space via a VDI 26 dBi diagonal horn antenna WR3.4DH. Using a calibrated pyroelectric detector, the power at the horn antenna aperture of the 120 Gbit/s transmission signal with pre-emphasis applied was measured to be -16.2 dBm. Two plano-convex 3" diameter PTFE lenses with 115 mm focal length were used to align the beam by collimating the output of the radiation from the emitter onto the reflecting mirrors and focusing the radiation into the receive horn antenna for block downconversion of

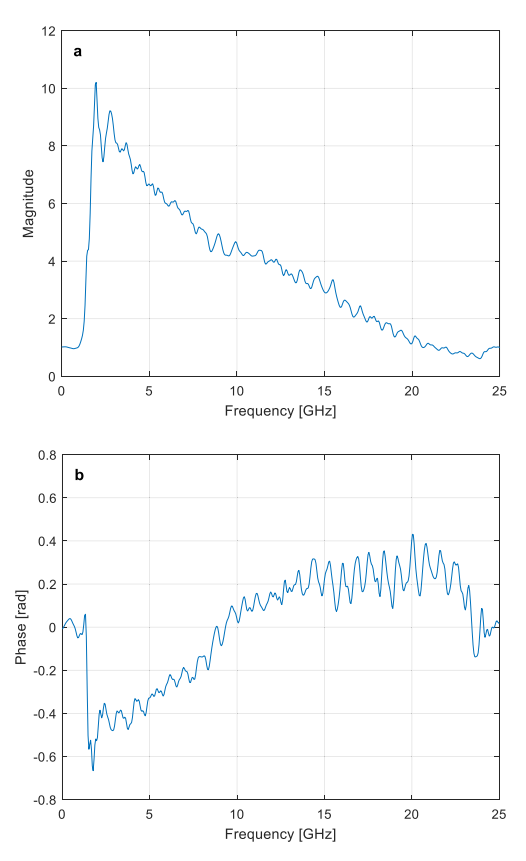


FIGURE 5. Testbed calibration results. The (a) magnitude and (b) phase of the correction function applied to the wideband AWG signals at the transmitter to pre-compensate for impairments in the transmission setup at 120 Gbit/s.

the transmitted data. The power of the transmitted signal directly in front of the receiver aperture was measured to be -24.5 dBm. A broadband linear amplifier (SHF S824 A) was



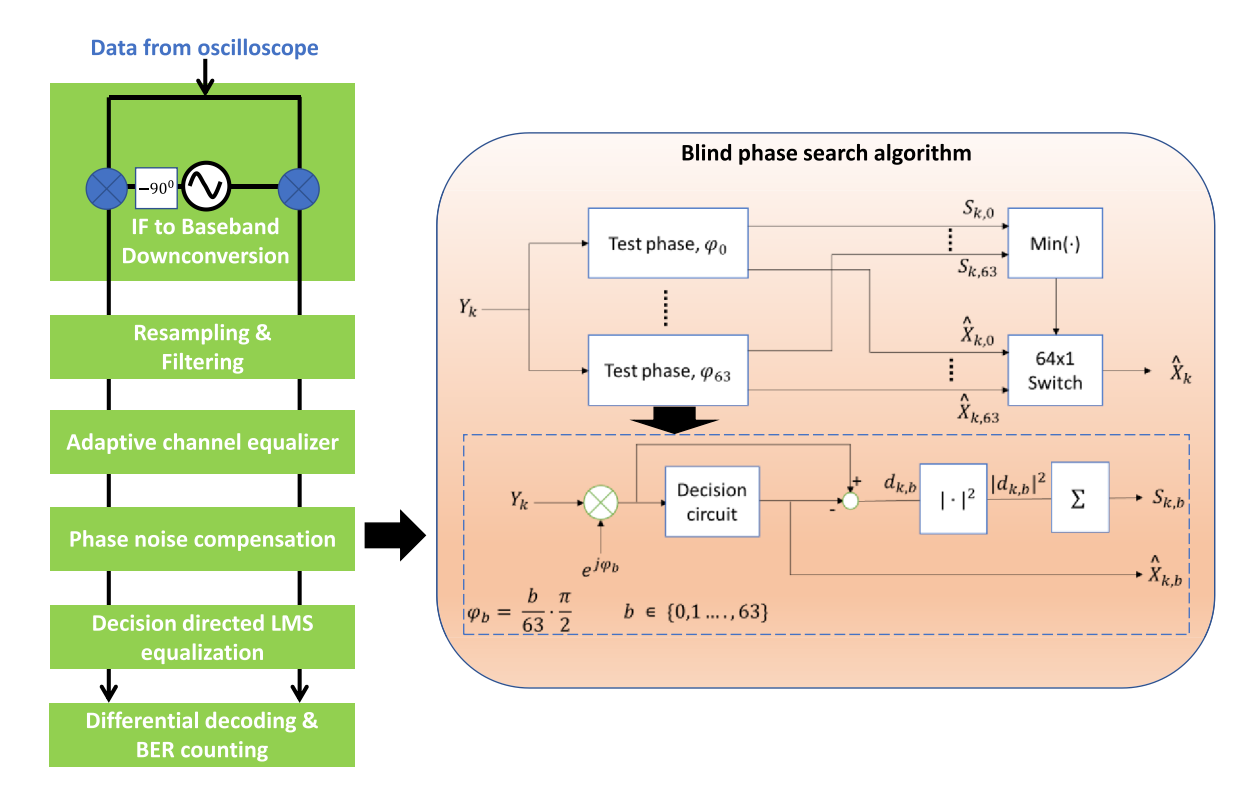


FIGURE 6. Digital Signal Processing. Representation of the DSP chain used at the receiver. The blind phase search algorithm used for LO phase noise compensation in the system is also shown. Y_k is the output complex data from the adaptive channel equalizer block for phase noise compensation. The symbols are rotated by 64 test phase angles, φ_b , and fed into a decision circuit to compute the squared distance to the closest constellation point which are summed up to mitigate the impact of additive white Gaussian noise (AWGN) in the phase estimation process. The output symbol, \hat{X}_k , is selected by a switch controlled by the index of the minimum distance sum corresponding to the optimum phase angle. \hat{X}_k is the phase noise compensated data from the blind phase search algorithm to be fed to the DD-LMS equalization block before differential decoding and BER counting.

used at the VDI downconverter output to improve the SNR of the received signals. The amplifier output was connected to the Keysight UXR0704A real-time oscilloscope to capture the downconverted signal. The oscilloscope has a sampling rate of 256 GSa/s per channel and an analog bandwidth of 70 GHz with 10-bit analog to digital converter (ADC) vertical resolution.

To generate high-quality waveforms for high-speed data transmission, the AWG non-ideal frequency response was compensated through pre-distortion. In addition, robust channel estimation and equalization become increasingly challenging in low SNR environments with significant channel impairments. Therefore, to compensate the channel impairments of the THz-wireless link as well as the combined effects of hardware amplitude and phase impairments, we characterized the system for pre-emphasis equalization on the transmitted waveform and then applied post-transmission offline Digital Signal Processing (DSP) on the received signal as described in the next section. The characterization of the system for pre-emphasis equalization was essential to demonstrate transmission of higher-order quadrature amplitude modulation schemes such as 64-QAM (see Appendix). Figure 5 shows the magnitude and phase of the correction function used for pre-emphasis equalization on the AWG modulated signal for transmission at 120 Gbit/s. The calibration process was repeated at different baud rates to create the corresponding correction functions for data transmission in the 300 GHz band.

IV. POST-TRANSMISSION DIGITAL SIGNAL PROCESSING

At the receive end, the IF modulated signals were digitized by the 256 GSa/s real-time oscilloscope UXR0704A and fed to DSP functional blocks for subsequent offline processing. The DSP schemes used to compensate the channel impairments for the wireless link and signal demodulation are shown in Figure 6. To evaluate the performance of the transmitted data stream, we calculate the BER through error counting which is regarded as the most conclusive figure of merit for the 300 GHz transmission link.

In the DSP routine, a digital mixer was used to down-convert the received digital signal to baseband and extract the *I*- and *Q*-channels for 64-QAM demodulation. After down-conversion, the baseband signal is processed through resampling and matched filtering. We then applied a *T/2*-spaced adaptive constant modulus algorithm (CMA) equalizer with 7 taps to compensate for channel impairments and hardware limitations [30]. Phase noise level from the LO can be a significant factor that inhibits the 64-QAM demodulation in the 300 GHz band. We used the blind phase search algorithm to compensate for the phase noise in the

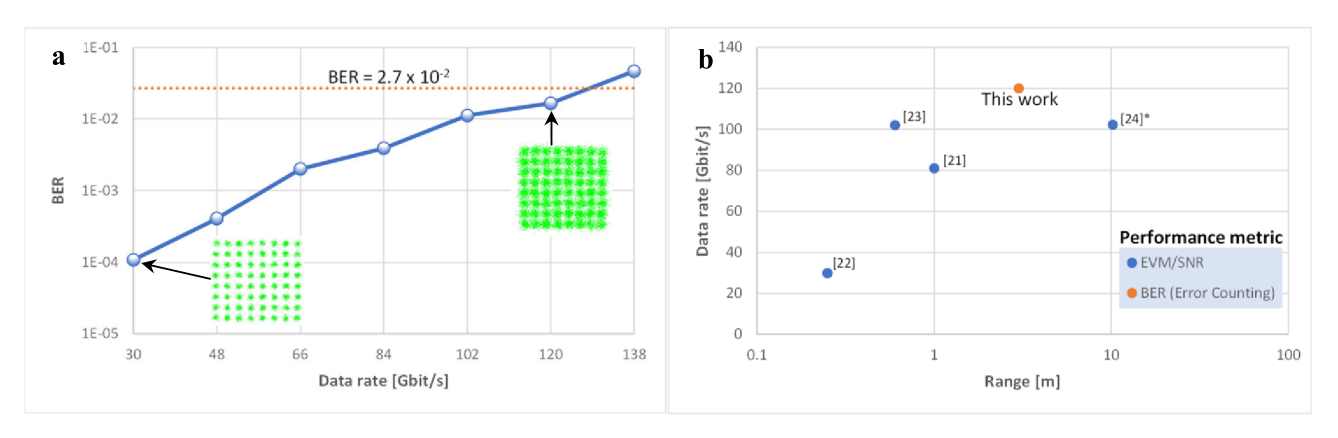


FIGURE 7. Transmission results. (a) The BER performance at different data rates over a 3 m NLoS wireless distance. The BER is under the SD-FEC of 2.7×10^{-2} up to 120 Gbit/s. The insets show the recovered 64-QAM constellations at 30 Gbit/s and 120 Gbit/s. (b) A comparison of reported 64-QAM data rates versus link distances using state-of-the-art electronics-based transmitters above 200 GHz with BER, EVM or SNR used as performance metric. *equivalent link distance estimated from SNR.

transmission system [31]. Here, 64 test phase angles were used in the blind phase search algorithm for carrier phase recovery as depicted in Figure 6. Following phase noise compensation, we employed a *T*-spaced decision-directed least-mean-square (DD-LMS) feedforward equalizer with 7 taps before finally computing the BER through differential decoding and error counting over 120,000 transmitted bits (20,000 64-QAM symbols).

V. 64-QAM TRANSMISSION RESULTS AND DISCUSSION

Using the testbed shown in Figure 3, we evaluated the 64-QAM transmission performance over 3 m wireless link using 26 dBi horn antennas, PTFE lenses and reflections through 2 mirrors in the setup. To reduce the spectral spread of the signal and fit within the transmission hardware bandwidth, a root raised cosine filter was applied for pulse shaping to the AWG data stream at the transmitter followed by matched filtering at the receiver in the DSP routine. The full electronic wireless link demonstration has been realized using commercially available upconverter and downconverter in the 300 GHz band. Using sub-harmonic mixers to generate the high frequency signals, linear behavior essential for 64-QAM transmission can be obtained. Also, the impact of several impairments was minimized following the system characterization procedure using the Vector Signal Analysis (VSA) and IQ Tools software for pre-emphasis equalization prior to data transmission (see Appendix).

The transmission results of the 64-QAM wireless link are shown in Figure 7(a) from 30 to 138 Gbit/s. The recovered signal constellations are also presented in Figure 7(a) as insets at 30 Gbit/s and 120 Gbit/s. To evaluate the bit error ratio (BER) performance of the transmission system, the data captured from the real-time oscilloscope was analyzed using the DSP chain shown in Figure 6. The measured BER up to 120 Gbit/s was under the SD-FEC threshold of 2.7×10^{-2} where error-free transmission can be achieved with 20% overhead giving a net data rate of 100 Gbit/s post-FEC [32]. Our transmission results demonstrate that thorough

characterizations of the testbed significantly improve link capacity and system performance. To the best of our knowledge, the 120-Gbit/s single-carrier modulated wireless transmission presented in this paper is the highest data rate reported above the 200-GHz-band transmission for 64-QAM modulation scheme using all electronics-based approach as compared in Figure 7(b). It is worth noting that instead of using EVM or SNR estimators to evaluate the performance of the 300 GHz transmission link, we implemented BER counting in this demonstration as the most conclusive figure of merit for the 64-QAM transmission. This is particularly important when the recovered 64-QAM constellation is distorted or corrupted by phase and multiplicative white noise sources leading to constellation points which are not perfectly circular [33]. In such scenarios, EVM and SNR estimators can lead to inaccurate performance evaluation of the transmission link compared to direct BER counting.

In our experiments, we employed a pair of lenses to collimate the transmission beam and reduce the free space propagation loss in the 3 m communication link. However, it is noteworthy that on-chip antenna with Si lens has also been demonstrated and can replace PTFE lenses for a more compact solution [34]. The on-chip antenna with Si lens provides a highly integrated, robust and precommercial subcomponent for THz transceivers. Noting this and anticipating further progress in the field, such as in-line sub-THz amplification, we expect transmission over hundreds of metres in the foreseeable future using commercial off-theshelf electronics-based transceivers and 64-QAM modulation scheme as investigated in this paper to increase data capacity in the THz band well beyond 100 Gbit/s and eventually towards Tb/s. Moreover, using multiple reflections for NLoS communications as demonstrated in this work for THz wireless link paves the way for several potential applications requiring high-throughput transmission system by employing intelligent reflecting surfaces (IRS) which are being actively investigated for the prospective 6G wireless systems [35].



VI. STANDARDIZATION EFFORT

The 300 GHz band is attracting significant attention as a key enabler for beyond-5G wireless communication systems promising over an order of magnitude greater capacity compared to existing wireless solutions operating within lower frequency bands. In response to such growing interest, new standards and regulations are emerging and the IEEE Std. 802.15.3d amendment is a notable example [36], [37]. It is the first world-wide standard, in the field of terahertz communications, to support the operation of high-speed wireless links up to 100 Gbit/s. In this standard, the frequency range from 252 GHz to 321 GHz is dedicated to wireless communications providing a bandwidth of 69 GHz. The wide available bandwidth enables many future applications for ultra-high data rate links and supports point-to-point connectivity for distances ranging from tens of centimeters up to a few hundred meters. In addition, IEEE 802.15.3d also enables connectivity within the electronic components inside a single device. Here, the standard can provide an elegant solution to the rapid growth in the data exchange inside computers where modern motherboards already have up to 12 layers. Vertical components such as dual in-line memory modules on a computer motherboard, for example, can be used to create NLoS link at 300 GHz for ultrafast inter-chip data exchange [38]. The IEEE 802.15.3d standard paves the way for extremely-high-rate data pipes between critical components, while simultaneously simplifying the layout design. The NLoS 120 Gbit/s demonstration in this article aligns with the aim of the IEEE 802.15.3d standard to offer high-rate data exchange for a plethora of potential applications in the 300 GHz band.

VII. CONCLUSION

In summary, we have successfully demonstrated the achievement of a single channel NLoS transmission over 3 m using sub-harmonic mixers and 64-QAM modulation format. We demonstrated that an accurate correction of different error sources in the transmission setup such as channel impairments of the 300 GHz wireless link as well as the combined effects of hardware amplitude and phase impairments can be achieved for high spectral-efficiency modulation. The indoor wireless link has been validated up to 120 Gbit/s in the 300 GHz band with the BER performance below the SD-FEC threshold of 2.7×10^{-2} with 20% overhead. To the best of our knowledge, this is the highest 64-QAM data rate achieved using an electronics-based transmitter in the 300 GHz band with the performance evaluated through BER counting as the most conclusive performance metric for the testbed. Development of sub-THz amplifiers and high gain antennas, for instance, would further benefit this fully electronic system by increasing the transmission reach beyond 3 m. Finally, we discussed the standardization progress on the IEEE 802.15.3d standard where promising ideas and solutions are emerging to contribute to the commercial appearance of THz communications and form the basis for the prospective 6G wireless systems.

APPENDIX SYSTEM CHARACTERIZATION

In order to improve over-the-air (OTA) transmission performance, modern receivers integrate efficient algorithms to estimate channel impairments as well as the combined effects of hardware amplitude and phase impairments for correction. However, extending the transmission bandwidth in the THz bands exceeds the capabilities of today's algorithms to accurately recover high-order modulation formats. Novel, often AI-based, signal processing techniques targeting THz communications among other frequency bands are the subject of active research but not yet available in commercial test & measurement tools. The approach adopted here to achieve communications beyond 120 Gbit/s with 64-QAM modulation scheme in the 300 GHz band is therefore an iterative one. It is based on standard software tools that are well-established for wideband signal generation and analysis.

As a starting point, we set up a QPSK signal which is relatively straightforward to demodulate and recover the constellation using Keysight Technologies' IQ Tools. The software IQ Tools is a MATLAB® based user interface (UI) facilitating instrument control and signal creation for Keysight Technologies' AWG. As illustrated in Figure 3, the AWG sends the original waveform as an IF signal over the beam path and the received IF signal is captured with the real-time oscilloscope. Keysight Technologies' PathWave Vector Signal Analysis (VSA) software is then used to demodulate the signal to recover the constellation, eye diagram and EVM. The VSA software is a commercial tool to analyze a wide variety of standard compliant and user-defined modulation formats.

The digital demodulator implementation in the VSA software incorporates an adaptive finite impulse response feed-forward equalization filter compensating linear distortions from the signal. The equalization filter is initialized from the IQ Tools interface using the calibration process. The IQ Tools UI enables 3 key calibration parameters to be defined in our experiments: the central frequency, filter length and convergence. The central frequency is set to the IF frequency used for the waveform which was 13 GHz for the data provided within this paper except for the 23 GBaud (138 Gbit/s) signal where the IF was set to 15 GHz for optimum performance. The filter length parameter sets the length of the VSA equalization filter and may be set to any odd number between 3 and 99. For transmission in multi-path environments, a longer filter length should be used. As the beam path used in our experiments was 3 m OTA transmission and included lenses and mirrors with an amplifier between the receiver and oscilloscope, the maximum filter length of 99 was used. Finally, the convergence parameter determines the rate at which the equalization filter converges and the larger this value the faster the rate of convergence. However, if the convergence value is too large for a given signal, the algorithm used within the calibration routine can become unstable leading to distorted constellations. The optimum value for the convergence parameter was set to 10^{-8} in our experiments.



Once the parameters have been set and the calibration process has been started, the equalization filter will run continuously until optimal convergence has been reached. This is determined by closely monitoring the EVM value produced by the VSA software for its minimum value. At this stage, IQ Tools reads the filter coefficients from the VSA software compensating for channel and hardware impairments and then applies the corresponding correction to the original AWG waveform to be transmitted. When aiming to produce a signal at a bandwidth where a recognizable QPSK constellation cannot be achieved before the calibration procedure, we calibrated the signal at a lower bandwidth first. Maintaining the low-order modulation format, the signal bandwidth is progressively increased to the final desired value. Once the calibration process has been completed and a correction file can be generated and applied, the modulation order is increased to 64-QAM for optimal BER performance. The calibration process to generate the correction file is repeated at different baud rates to obtain the transmission results presented in Figure 7.

REFERENCES

- M. D. Al-Dabbagh, J. Smith, T. Kleine-Ostmann, M. Naftaly, and I. Fatadin, "Characterising the photonic-assisted coherent freespace link of sub-THz data transmission," *IEEE Access*, vol. 11, pp. 128081–128093, 2023, doi: 10.1109/ACCESS.2023.3332485.
- [2] D. Wrana, L. John, B. Schoch, S. Wagner, and I. Kallfass, "Sensitivity analysis of a 280–312 GHz superheterodyne terahertz link targeting IEEE802.15.3d applications," *IEEE Trans. THz Sci. Technol.*, vol. 12, no. 4, pp. 325–333, Jul. 2022, doi: 10.1109/TTHZ.2022.3172008.
- [3] H.-J. Song, "Terahertz wireless communications: Recent developments including a prototype system for short-range data downloading," *IEEE Microw. Mag.*, vol. 22, no. 5, pp. 88–99, May 2021, doi: 10.1109/MMM.2021.3056935.
- [4] L. Gonzalez-Guerrero, H. Shams, I. Fatadin, J. E. Wu, M. J. Fice, M. Naftaly, A. J. Seeds, and C. C. Renaud, "Pilot-tone assisted 16-QAM photonic wireless bridge operating at 250 GHz," *J. Lightw. Technol.*, vol. 39, no. 9, pp. 2725–2736, May 2021, doi: 10.1109/JLT.2021.3053616.
- [5] I. Dan, G. Ducournau, S. Hisatake, P. Szriftgiser, R.-P. Braun, and I. Kallfass, "A terahertz wireless communication link using a superheterodyne approach," *IEEE Trans. THz Sci. Technol.*, vol. 10, no. 1, pp. 32–43, Jan. 2020, doi: 10.1109/TTHZ.2019.2953647.
- [6] T. S. Rappaport, Y. Xing, O. Kanhere, S. Ju, A. Madanayake, S. Mandal, A. Alkhateeb, and G. C. Trichopoulos, "Wireless communications and applications above 100 GHz: Opportunities and challenges for 6G and beyond," *IEEE Access*, vol. 7, pp. 78729–78757, 2019, doi: 10.1109/ACCESS.2019.2921522.
- [7] H. Elayan, O. Amin, B. Shihada, R. M. Shubair, and M.-S. Alouini, "Terahertz band: The last piece of RF spectrum puzzle for communication systems," *IEEE Open J. Commun. Soc.*, vol. 1, pp. 1–32, 2020, doi: 10.1109/OJCOMS.2019.2953633.
- [8] M. F. Hermelo, P.-T. Shih, M. Steeg, A. Ng'oma, and A. Stöhr, "Spectral efficient 64-QAM-OFDM terahertz communication link," *Opt. Exp.*, vol. 25, no. 16, p. 19360, Aug. 2017.
- [9] S. Jia, M.-C. Lo, L. Zhang, O. Ozolins, A. Udalcovs, D. Kong, X. Pang, R. Guzman, X. Yu, S. Xiao, S. Popov, J. Chen, G. Carpintero, T. Morioka, H. Hu, and L. K. Oxenløwe, "Integrated dual-laser photonic chip for high-purity carrier generation enabling ultrafast terahertz wireless communications," *Nature Commun.*, vol. 13, no. 1, p. 1388, Mar. 2022, doi: 10.1038/s41467-022-29049-2.
- [10] J. D. Preez, S. Sinha, and K. Sengupta, "SiGe and CMOS technology for state-of-the-art millimeter-wave transceivers," *IEEE Access*, vol. 11, pp. 55596–55617, 2023, doi: 10.1109/ACCESS.2023.3282693.
- [11] H. Ito, T. Furuta, Y. Muramoto, T. Ito, and T. Ishibashi, "Photonic millimetre- and sub-millimetre-wave generation using J-band rectangularwaveguide-output uni-travelling-carrier photodiode module," *Electron. Lett.*, vol. 42, no. 24, p. 1424, 2006.

- [12] T. Ishibashi, Y. Muramoto, T. Yoshimatsu, and H. Ito, "Unitraveling-carrier photodiodes for terahertz applications," *IEEE J. Sel. Topics Quantum Electron.*, vol. 20, no. 6, pp. 79–88, Nov. 2014.
- [13] C. Castro, R. Elschner, T. Merkle, C. Schubert, and R. Freund, "Experimental demonstrations of high-capacity THz-wireless transmission systems for beyond 5G," *IEEE Commun. Mag.*, vol. 58, no. 11, pp. 41–47, Nov. 2020, doi: 10.1109/MCOM.001.2000306.
- [14] P. Rodríguez-Vázquez, J. Grzyb, N. Sarmah, B. Heinemann, and U. R. Pfeiffer, "Towards 100 gbps: A fully electronic 90 gbps one meter wireless link at 230 GHz," in *Proc. 15th Eur. Radar Conf. (EuRAD)*, Sep. 2018, pp. 369–372.
- [15] S. Lee, "An 80Gb/s 300 GHz-band single-chip CMOS transceiver," IEEE J. Solid-State Circuits, vol. 54, no. 12, pp. 3577–3588, Dec. 2019.
- [16] H. Hamada, T. Fujimura, I. Abdo, K. Okada, H.-J. Song, H. Sugiyama, H. Matsuzaki, and H. Nosaka, "300-GHz. 100-Gb/s InP-HEMT wireless transceiver using a 300-GHz fundamental mixer," in *IEEE MTT-S Int. Microw. Symp. Dig.*, Jun. 2018, pp. 1480–1483.
- [17] P. Rodriguez-Vazquez, J. Grzyb, B. Heinemann, and U. R. Pfeiffer, "A QPSK 110-Gb/s polarization-diversity MIMO wireless link with a 220–255 GHz tunable LO in a SiGe HBT technology," *IEEE Trans. Microw. Theory Techn.*, vol. 68, no. 9, pp. 3834–3851, Sep. 2020, doi: 10.1109/TMTT.2020.2986196.
- [18] K. K. Tokgoz, S. Maki, J. Pang, N. Nagashima, I. Abdo, S. Kawai, T. Fujimura, Y. Kawano, T. Suzuki, T. Iwai, K. Okada, and A. Matsuzawa, "A 120Gb/s 16QAM CMOS millimeter-wave wireless transceiver," in IEEE Int. Solid-State Circuits Conf. (ISSCC) Dig. Tech. Papers, Feb. 2018, pp. 168–170.
- [19] C.-L. Cheng and A. Zajic, "Characterization of propagation phenomena relevant for 300 GHz wireless data center links," *IEEE Trans. Antennas Propag.*, vol. 68, no. 2, pp. 1074–1087, Feb. 2020, doi: 10.1109/TAP.2019.2949135.
- [20] N. Boujnah, S. Ghafoor, and A. Davy, "Modeling and link quality assessment of THz network within data center," in *Proc. Eur. Conf. Netw. Commun. (EuCNC)*, Valencia, Spain, Jun. 2019, pp. 57–62, doi: 10.1109/EuCNC.2019.8801998.
- [21] P. Rodríguez-Vázquez, J. Grzyb, B. Heineman, and U. R. Pfeiffer, "Optimization and performance limits of a 64-QAM wireless communication link at 220-260 GHz in a SiGe HBT technology," in *Proc. IEEE Radio Wireless Symp. (RWS)*, Orlando, FL, USA, Jan. 2019, pp. 1–3, doi: 10.1109/RWS.2019.8714283.
- [22] I. Abdo, H. Hamada, H. Nosaka, A. Shirane, and K. Okada, "64 QAM wireless link with 300 GHz InP-CMOS hybrid transceiver," *IEICE Electron. Exp.*, vol. 18, no. 17, pp. 1–4, 2021.
- [23] Z. Lai, C. Li, Y. Li, X. Lai, J. Li, and K. Guan, "A high-order modulation (64-QAM) broadband THz communication system over 100 gbps," in *Proc. IEEE 4th Int. Conf. Electron. Inf. Commun. Technol. (ICEICT)*, China, Aug. 2021, pp. 553–556, doi: 10.1109/ICE-ICT53123.2021.9531263.
- [24] H. Hamada, T. Tsutsumi, H. Matsuzaki, T. Fujimura, I. Abdo, A. Shirane, K. Okada, G. Itami, H.-J. Song, H. Sugiyama, and H. Nosaka, "300-GHz-Band 120-Gb/s wireless front-end based on InP-HEMT PAs and mixers," *IEEE J. Solid-State Circuits*, vol. 55, no. 9, pp. 2316–2335, Sep. 2020, doi: 10.1109/JSSC.2020.3005818.
- [25] C. E. Shannon, "Communication in the presence of noise," Proc. IRE, vol. 37, no. 1, pp. 10–21, Jan. 1949.
- [26] C. Castro, R. Elschner, T. Merkle, C. Schubert, and R. Freund, "Long-range high-speed THz-wireless transmission in the 300 GHz band," in *Proc. 3rd Int. Workshop Mobile THz Syst. (IWMTS)*, Jul. 2020, pp. 1–4, doi: 10.1109/IWMTS49292.2020.9166263.
- [27] I. Kallfass, I. Dan, S. Rey, P. Harati, J. Antes, A. Tessmann, S. Wagner, M. Kuri, R. Weber, H. Massler, A. Leuther, T. Merkle, and T. Kürner, "Towards MMIC-based 300GHz indoor wireless communication systems," *IEICE Trans. Electron.*, vol. E98.C, no. 12, pp. 1081–1090, 2015, doi: 10.1587/transele.e98.c.1081.
- [28] L. John, A. Tessmann, A. Leuther, P. Neininger, T. Merkle, and T. Zwick, "Broadband 300-GHz power amplifier MMICs in InGaAs mHEMT technology," *IEEE Trans. THz Sci. Technol.*, vol. 10, no. 3, pp. 309–320, May 2020, doi: 10.1109/TTHZ.2020.2965808.
- [29] B. Schoch, A. Tessmann, A. Leuther, S. Wagner, and I. Kallfass, "300 GHz broadband power amplifier with 508 GHz gain-bandwidth product and 8 dBm output power," in *IEEE MTT-S Int. Microw. Symp. Dig.*, Jun. 2019, pp. 1249–1252.



- [30] I. Fatadin, D. Ives, and S. J. Savory, "Blind equalization and carrier phase recovery in a 16-QAM optical coherent system," *J. Lightw. Technol.*, vol. 27, no. 15, pp. 3042–3049, Aug. 1, 2009, doi: 10.1109/jlt.2009.2021961.
- [31] T. Pfau, S. Hoffmann, and R. Noe, "Hardware-efficient coherent digital receiver concept with feedforward carrier recovery for M-QAM constellations," J. Lightw. Technol., vol. 27, no. 8, pp. 989–999, Apr. 2009, doi: 10.1109/jlt.2008.2010511.
- [32] D. Chang, "LDPC convolutional codes using layered decoding algorithm for high speed coherent optical transmission," in *Proc. Opt. Fiber Commun. Conf. (OFC)*, Mar. 2012, pp. 1–3.
- [33] J. Chen, D. Kuylenstierna, S. E. Gunnarsson, Z. S. He, T. Eriksson, T. Swahn, and H. Zirath, "Influence of white LO noise on wideband communication," *IEEE Trans. Microw. Theory Techn.*, vol. 66, no. 7, pp. 3349–3359, Jul. 2018, doi: 10.1109/TMTT.2018.2814040.
- [34] P. Rodríguez-Vázquez, J. Grzyb, B. Heinemann, and U. R. Pfeiffer, "A 16-QAM 100-Gb/s 1-M wireless link with an EVM of 17% at 230 GHz in an SiGe technology," *IEEE Microw. Wireless Compon. Lett.*, vol. 29, no. 4, pp. 297–299, Apr. 2019.
- [35] Z. Chen, B. Ning, C. Han, Z. Tian, and S. Li, "Intelligent reflecting surface assisted terahertz communications toward 6G," *IEEE Wireless Commun.*, vol. 28, no. 6, pp. 110–117, Dec. 2021, doi: 10.1109/MWC.001.2100215.
- [36] IEEE Standard for High Data Rate Wireless Multi-Media Networks—Amendment 2: 100 Gb/s Wireless Switched Point-to-Point Physical Layer, Standard 802.15.3d-2017, 2017, pp. 1–55, doi: 10.1109/IEEESTD.2017.8066476.
- [37] V. Petrov, T. Kurner, and I. Hosako, "IEEE 802.15.3d: First standardization efforts for sub-terahertz band communications toward 6G," *IEEE Commun. Mag.*, vol. 58, no. 11, pp. 28–33, Nov. 2020, doi: 10.1109/MCOM.001.2000273.
- [38] S. Kim and A. Zajic, "Characterization of 300-GHz wireless channel on a computer motherboard," *IEEE Trans. Antennas Propag.*, vol. 64, no. 12, pp. 5411–5423, Dec. 2016, doi: 10.1109/TAP.2016.2620598.

IRSHAAD FATADIN (Senior Member, IEEE) is currently a Principal Scientist with the Electromagnetic Technologies Group, National Physical Laboratory (NPL). He is also a Visiting Professor with the Faculty of Engineering and Physical Sciences, University of Surrey. He leads NPL's collaborative research with industry and academia on several projects in the telecoms area. He is a Chartered Physicist (C.Phys.) and a Chartered Engineer (C.Eng.) registered with the Engineering Council, U.K.

JESS SMITH received the Ph.D. degree from the University of Surrey and the National Physical Laboratory (NPL), with a focus on scanning near-field optical microscopy (SNOM) and THz source characterization. She has been a Higher Scientist with the NPL, since 2022. Her current research interests include telecoms applications, including THz communications, antenna characterization, and mobile networks.

YUNSONG GUI received the master's degree in electromagnetic field and microwave from Shanghai Jiao Tong University, China, in 2006. In 2020, he joined the National Physical Laboratory (NPL), Teddington, U.K., as a Senior Scientist. He has over 18 years of experience in wireless communication and RF system design and performance verification. He was a senior baseband and RF engineer with a global telecommunication supplier and a Senior Researcher with the Chinese Academy of Sciences. His current research interests include OTA testing for advanced wireless communication systems, wireless channel modeling, and mm-wave and THz technologies.

INGO NICKELEIT received the Dipl.-Ing. degree in electrical engineering from the Technical University of Munich. After that, he was a Design Engineer of satellite communication systems with ViCon Engineering, Germany. He is a Solution Expert with Keysight Technologies, focusing on the research and development of communication systems. Before joining Keysight, he has been with Mentor Graphics, as an Application Engineer and the Product Marketing Manager for mixed-signal/RF products.

JAE PARK received the bachelor's and master's degrees in electrical engineering from the University of Virginia, in 2011 and 2017, respectively. In 2011, he joined Virginia Diodes Inc. (VDI), as a RF Production Test Engineer. In 2013, he transitioned to a sales, marketing, and applications engineering position providing solutions and support for a wide range of millimeter-wave and terahertz applications.

JEFFREY L. HESLER (Fellow, IEEE) is the President and the Chief Technology Officer of Virginia Diodes Inc. He has been working on creating new technologies that utilize the terahertz (THz) frequency band for scientific, defense, and industrial applications, for more than 30 years. He has published over 200 technical papers in journals and international conference proceedings. He is a member of the IEEE Technical Committee MTT-21 (THz Technology and Applications). His innovative designs are currently used in hundreds of research laboratories throughout the world. He is a Co-Editor of IEEE Transactions on Terahertz Science and Technology.

...